Experimental Study of the Course of Threshold Current, Voltage and Electrode Impedance During Stepwise Stimulation From the Skin Surface to the Human Cortex

Szelenyi, Andrea; Journee, Henricus Louis; Herrlich, Simon; Galistu, Gianni M.; van den Berg, Joris; van Dijk, J. Marc C.

Published in:
Brain stimulation

DOI:
10.1016/j.brs.2012.10.002

Publication date:
2013

Brain Stimulation 6 (2013) 482–489

Contents lists available at SciVerse ScienceDirect

Brain Stimulation

journal homepage: www.brainstimjrnl.com

Experimental Study of the Course of Threshold Current, Voltage and Electrode Impedance During Stepwise Stimulation From the Skin Surface to the Human Cortex

Andrea Szelényi [a,*,1], Henricus Louis Journée [b,c,1], Simon Herrlich [d], Gianni M. Galistu [b], Joris van den Berg [e], J. Marc C. van Dijk [b]

[a] Department for Neurosurgery, Johann Wolfgang Goethe-University Hospital, Frankfurt a. M., Germany[2]
[b] Department of Neurosurgery, University Medical Center Groningen, Groningen, The Netherlands
[c] Department for Orthopedics, Sint Maartenskliniek, Nijmegen, The Netherlands
[d] Laboratory for Biomedical Microtechnology, Department of Microsystems Engineering, IMTEK, University of Freiburg, Germany
[e] Medical Engineering and Service Department, Sint Maartenskliniek, Nijmegen, The Netherlands

ARTICLE INFO

Article history:
Received 30 January 2012
Received in revised form
30 September 2012
Accepted 6 October 2012
Available online 6 November 2012

Keywords:
Direct cortical stimulation
Transcranial stimulation
Motor evoked potential
Impedance
Skull
Scalp
Brain
Voltage stimulation
Current stimulation

ABSTRACT

Background: Transcranial electric stimulation as used during intraoperative neurostimulation is dependent on electrode and skull impedances.
Objective: Threshold currents, voltages and electrode impedances were evaluated with electrical stimulation at 8 successive layers between the skin and the cerebral cortex.
Patients and Methods: Data of 10 patients (6f, 53 ± 11 years) were analyzed. Motor evoked potentials were elicited by constant current stimulation with corkscrew type electrodes (CS) at C3 and C4 in line with standard transcranial electric stimulation. A monopolar anodal ball tip shaped probe was used for all other measurements being performed at the level of the skin, dura and cortex, as well as within the skull by stepwise performed burr holes close to C3 resp. C4.
Results: Average stimulation intensity, corresponding voltage and impedance for muscle MEPs at current motor threshold (CMT) were recorded: CS 54 ± 23 mA (mean ± SD), 38 ± 21 V, 686 ± 146 Ω; with the monopolar probe on skin 55 ± 28 mA, 100 ± 44 V, 1911 ± 683 Ω and scalp 59 ± 32 mA, 56 ± 28 V, 1010 ± 402 Ω; within the skull bone: outer compact layer 33 ± 23 mA, 91 ± 53 V, 3734 ± 2793 Ω; spongiform layer 33 ± 23 mA, 70 ± 44 V, 2347 ± 1327 Ω; inner compact layer (ICL) 28 ± 19 mA, 48 ± 23 V, 2103 ± 1498 Ω; on dura 25 ± 12 mA, 17 ± 12 V, 643 ± 244 Ω and cortex 14 ± 6 mA, 11 ± 5 V, 859 ± 300 Ω. CMTs were only significantly different for CS ($P = 0.02$) and for the monopolar probe between the cortex and ICL ($P = 0.03$), scalp ($P = 0.01$) or skin ($P = 0.01$) and between ICL and CS ($P \leq 0.01$) or skin ($P \leq 0.01$).
Conclusion: The mean stimulation current of the CMT along the extracranial to intracranial anodal trajectory followed a stepwise reduction. VMT was strongly dependent on electrode impedance. CMT within the skull layers was noted to have relative strong shunting currents in scalp layers.

Introduction

Motor evoked potentials (MEPs) elicited by transcranial electric stimulation (TES) are widely used for intraoperative assessment of the motor cortex and motor pathways [1–7]. To overcome effects of anesthesia, pulse series of high frequency trains (commonly 5 pulses applied with an interstimulus interval of 4 ms) are used to elicit MEPs [8]. TES is not only dependent on vital parameters such as hypotension, but also on depth and type of anesthesia. Also, TES is reliant on the type of stimulator (voltage or constant current driven), stimulation parameters (stimulation frequency, pulse repetition and pulse duration) and the impedance of the stimulating electrodes. Finally, the conductivity and geometry of the structures being stimulated, e.g. the skull, and the orientation and location of axons within the white matter, are factors of influence [9].

Together, these factors determine the stimulation intensity needed in order to eliciting MEPs and thus the motor thresholds (MT) [10–12]. In clinical practice, stimulation parameters are the easiest to control and assess. The physiological principle and empirically obtained stimulation parameters regarding constant

Funding: This work was supported by Inomed Co., Emmendingen, Germany in providing a travel grant to Simon Herrlich and technical support, which essentially made the study possible.
* Corresponding author. Department of Neurosurgery, University Hospital Duesseldorf, Moorenstrasse 5, D-40225 Duesseldorf, Germany. Tel.: +49 211 81 17646.
E-mail address: Andrea.Szelenyi@uni-duesseldorf.de (A. Szelényi).
[1] Both authors contributed equally to the paper.
[2] Institution where the work was performed.

1935-861X/$ – see front matter © 2013 Elsevier Inc. All rights reserved.
http://dx.doi.org/10.1016/j.brs.2012.10.002

current stimulation and thus obtained motor thresholds (CMT) for intraoperative TES have been established [13–15]. For intraoperative monitoring, not only the presence and absence of MEPs are used, but also the shift of motor thresholds during the operative procedure. At the same time, motor thresholds obtained by constant voltage driven stimulators (VMT) are also used as measurement for potentially harmful events [6,16].

VMT is more sensitive to local electrode impedance than CMT, although in the case of large contact areas, VMT is uncorrelated to electrode impedance due to minimal electrode impedance [12]. Corkscrew (CS) and needle electrodes – both predominantly used for practical reasons – have impedances above 460 Ω, whereas VMT is linearly related to the electrode impedance [12]. Therefore, local electrode impedance is mainly dependent on the contact surface of the electrode and specific conductance of surrounding scalp and skin tissues. In this perspective, particularly the human skull is known as a relative barrier for stimulation currents. When compared to other tissue layers, the specific impedance of the human skull is relatively high as measured by in-vitro experiments [17,18] or calculated by modeling [19,20]. These studies however, are based on assumptions of linearity at small signal intensities as non-linear conditions in vivo have not been identified to date.

Regarding shunting currents towards areas with higher conductivity (e.g. skin, cerebrospinal fluid (CSF)) CMT is more sensitive than VMT, which implies a variable distribution of stimulation current. In individual patients, shunting currents can be controlled to some degree by the type of stimulation electrodes and their placement. Stimulation thresholds decrease when the distance between electrodes increases or if current shunting decreases. To reduce current shunting through the scalp, it has been suggested to place electrodes within the skull (e.g. with screws), resulting in lower CMT [21]. This placement however comes with the price of an increased risk of infection. Furthermore, CMT is influenced by skull and subdural CSF conductivities nevertheless. Direct cortical stimulation excludes the aforementioned shunting currents through scalp and skull. Direct cortical anodal stimulation reduces CMT to 5–33 mA [22–24]. Depending on the type of surgery, direct stimulation of the cortex is not always possible. Thus knowledge of the electrical properties of TES is useful.

This study is designed to evaluate the course of CMT, VMT and electrode impedance during in vivo stepwise stimulation at 8 successive layers along a tract between the skin surface and cerebral cortex in humans.

Patients and methods

Patients

Patients were eligible for the study if they underwent intracranial tumor surgery, for which the craniotomy required a burr hole placed at C4 or C3 (electrode positions according to the international 10-20-EEG-coordination system) or within less than 1 cm distance from C4 or C3. The protocol prescribed that no additional burr hole was required for the craniotomy. Patients with motor impairment, implanted devices (e.g. cochlear implant, cardiac pacemaker) or frequent epileptic seizures were excluded from the study. The study was approved by the local medical-ethical committee and written informed consent was obtained from all patients prior to surgery.

Methods

Anesthesia

After anesthetic induction with a bolus of Disoprivan (1.5–2 mg/kg), Remifentanil (1 μg/kg) and the medium duration acting muscle relaxant Rocuronium (50 mg bolus) for intubation only the electrodes were attached to the patient. Anesthesia was further maintained with Disoprivan (4–6 mg/kg × h) and Remifentanil (0.2–0.4 μg/kg × min).

Stimulation

Stimulation electrodes: for TES, corkscrew type-electrodes (CS, CareFusion, Höchberg, Germany) were placed at C3 and C4. For left hemispheric stimulation, C3 served as anode referenced to C4 serving as cathode, for right hemispheric stimulation C4 served as anode referenced to C3 serving as cathode. For all other stimulation, a monopolar straight stimulation probe with a ball tip electrode of 0.2 cm diameter (BCS-ball tip electrode, Inomed Co., Emmendingen, Germany) was used. This monopolar probe served as anode, the contralateral CS electrode served as cathode. Stimulation was performed with a constant current stimulator (Osiris, Inomed Co., Emmendingen, Germany) delivering an undistorted rectangular pulse (even when using complex load impedances) with a maximum output of 220 mA and a voltage range up to 300 V. According to previously published methodology and to reliably eliciting MEPs, a train of five stimuli with an individual pulse width of 0.5 ms and an interstimulus interval of 4 ms at a 0.5 Hz repetition rate was used [8,15]. By increasing the stimulation intensity stepwise, the motor threshold of eliciting reproducible MEPs of 50 μV amplitude was determined.

Recording parameters

MEPs were obtained from the contralateral abductor pollicis brevis muscle using pairs of subdermal needle electrodes. The response was recorded with a band width of 10–1000 Hz and a 160 ms epoch length.

Set-up

To measure the electrical properties of electrical stimulation (TES and direct cortical stimulation), the technical set-up was as follows: the stimulating electrodes (CS and the stimulating probe) were connected to the stimulator by a circuit comprising a shunt resistor (R_{shunt}; 10 Ω, accuracy of 1%) for current measurements (Fig. 1). The voltage over the stimulating electrodes and R_{shunt} is measured by the two channel digital PC-oscilloscope (DS1M12, Meilhaus Electronic, Munich, Germany). Digitizing was performed by a 1 MHz sampling rate for repetitively performed measurements. The impedance of the measuring probe was either 1 or 10 M-Ohm depending on the required voltage range of the oscilloscope input. The stimulation intensity (I, [mA]) and the voltage (V, [V]) of the first pulse of the train of five were analyzed to avoid inaccuracies introduced by build-up effects from repeated stimuli in pulse trains [25]. The impedance between the stimulating electrodes (R_{el}, [Ω]) was computed according to Ohm's law ($R_{el} = V/I$). The measurements were performed twice for reproducibility checks. CMT and VMT are the values of respectively I and V at motor threshold stimulus intensities. VMT is read from the mid-pulse voltage that is measured simultaneously with the mid-pulse current at the current threshold condition that defines CMT.

Study protocol

After induction of anesthesia, stimulating and recording electrodes were attached to the patient. Intraoperative neuromonitoring consisted of somatosensory evoked potentials and MEPs. For both, recordings were taken after patient's positioning. Once those were recorded, measurements for this study were taken in the following work-flow (see Fig. 2 for illustration). MEPs were elicited first with the CS-electrode montage C3-anode/C4-cathode and vice versa. Afterward, the CS electrode within the surgical field was removed while the remaining electrode still served as

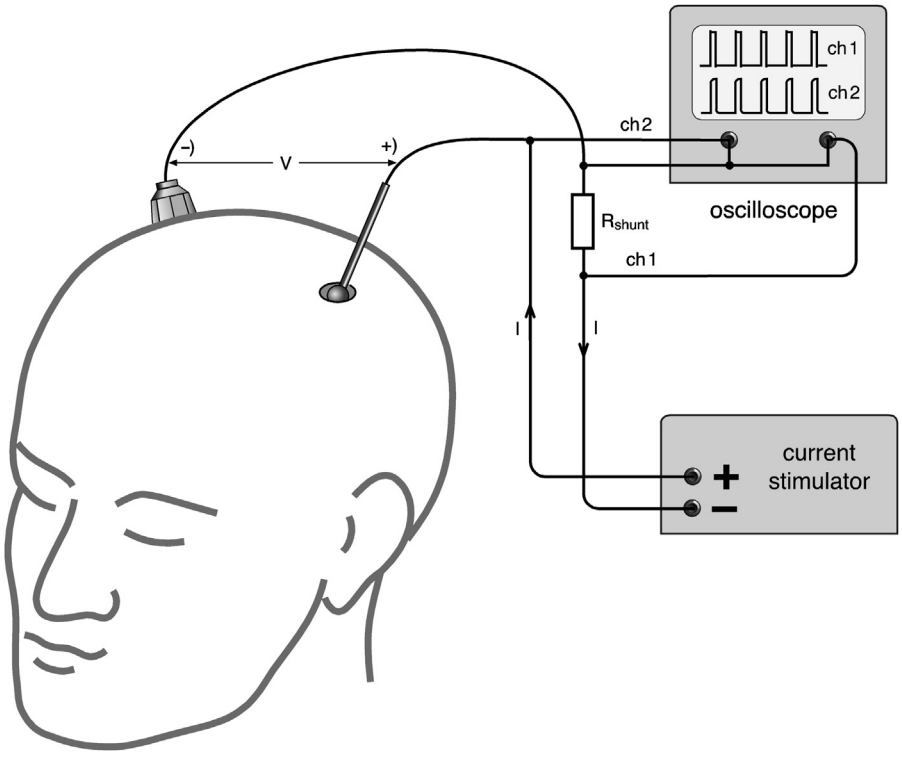

Figure 1. Schematic diagram of the set-up for simultaneous measurements of the stimulation potential and currents of a train of five monophasic stimulation pulses for elicitation of motor potentials. A corkscrew electrode (CS) is placed at C4. An anodal ball-tip electrode is shown at the entrance of the tract from the skin to the cortex of the brain of the measurements at C3. The stimulation potential is measured at channel 2 (Ch. 2) of the oscilloscope. The stimulation current (I) of the pulse trains is measured by channel 1 (Ch. 1) as a potential, V, over the shunt resistor R_{shunt} ($R_{shunt} = 10\ \Omega$ (1%); sensitivity: $I = 0.1 \times V$ where the current I is flows through R_{shunt} and the voltage V is measured across R_{shunt}). The arrows indicate the direction of the current during stimulation.

cathode. The measurements were continued using the monopolar stimulating probe and were performed on the skin (1), at the spot of the removed CS electrode, and after incision at the same location within the skin of the scalp (2). After the skin flap was removed, the measurements were continued at the same position on the skull (3). Then, the surgeon drilled a 1-cm burr hole in a stepwise fashion with a common craniotom. While drilling, the surgeon estimated the depth for each layer within the skull and the measurements were performed at the following layers of the skull: outer compact layer (OCL, 4), spongiform layer (SL, 5) and inner compact layer (ICL, 6). The craniotomy was finalized and measurements were continued on the dura (epidural layer; ED, 7) and finally – if possible according to the dura opening on the cortex (8). In those patients, in which extensive cortical mapping for tumor removal was necessary, only stimulation intensities of direct cortical stimulation close to the burr hole were included. Such, extensive mapping for determining the hot spot (i.e. lowest stimulation intensity to elicit MEPs) of the contralateral abductor pollicis brevis muscle was only performed if necessary for tumor resection. At each step the measurement was performed twice to check the reproducibility. The bottom of the burr hole was kept moist with a drop of saline irrigation solution.

Data analysis

The accuracy of the stimulator was determined by calculating the mean difference of the individual value setting to the reading of the oscilloscope setting.

The visual analysis of the pulse form within the pulse trains did not show any build-up effect in current as well as the current series (Fig. 3).

Reproducibility of CMT, VMT and R_{el} were calculated as the mean reproducibility error (mRE) according to:

$$\mathrm{mRE} = (100/N)\sum_{i=1}^{N}(A_i - B_i)/(A_i + B_i)\%$$

A and B refer to the value of CMT_i, VMT_i or R_i (index "i" denotes the case number) of the first and second measurements at each level of the stepwise stimulation respectively. Statistical significance was tested by Student's t-test at a 0.05 level of significance. Because deviation between the first and second measurement can be positive or negative, a two tailed test was applied. Reproducibility of CMT within the truncation error of 1 mA allowed proceeding with further statistical analysis with the first of the two subsequent measurements for each tested layer only. To avoid underestimation of current values, data was excluded when recorded stimulation voltages exceeded 275 V. This allowed a 25 V buffer to the voltage limit of the current stimulator to avoid any clipping effects.

The degree to which CMTs of every of the 8 subsequent layers between the skin surface and the cerebral cortex correlated, was analyzed by a cross comparison (Student's t-test (paired) at 0.05 level of significance). The relation between R_{el}, VMT and CMT was analyzed with two-tailed Spearman's correlations for 0.05 and 0.01 significance levels.

Results

11 patients (6f, 5m, 54 ± 11 years) were studied after written informed consent was obtained (Table 1). Due to inverse polarity of the stimulating electrodes (accidentally cathodal instead of anodal

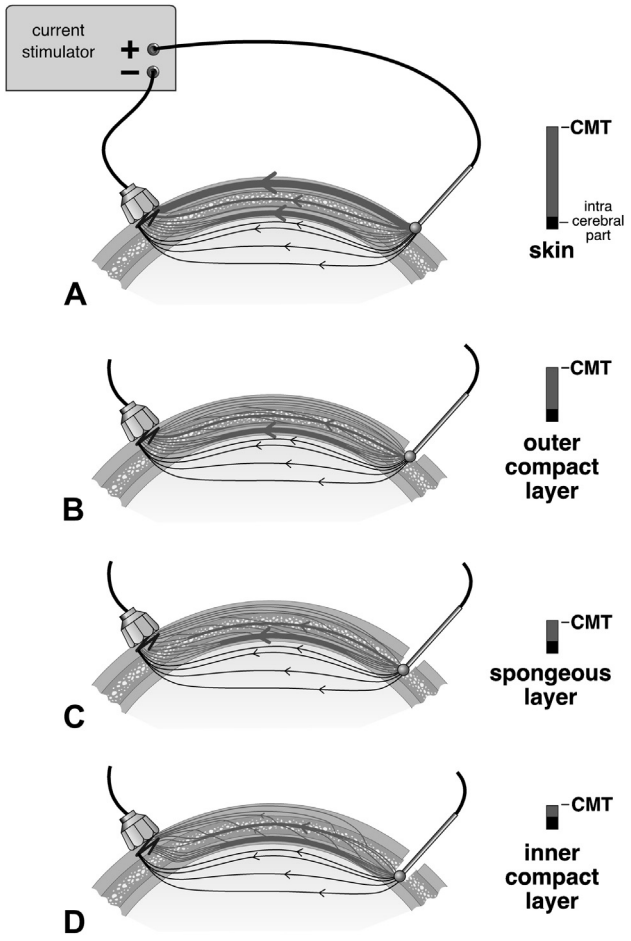

Figure 2. Schematic drawing of hypothetical courses of the current flow between a stimulating anodal ball tip electrode at C3 and a corkscrew electrode (cathode) at C4. The diagrams show four depths: (A) skin level and 3 skull layers: (B) outer compact layer, (C) spongiform layer and (D) at the inner compact layer. The stimulation is performed at threshold level for elicitation of MEPs in the contralateral abductor pollices brevis muscle. The thermometer at the right in each diagram shows the electrode current threshold CMT relative to the portion of the current through the brain (black). A marked decrease of CMT is expected from skin level to the outer compact layer due to the significant reduction of the shunting current through the good conducting scalp. The decrease is expected to be smaller at further burr-hole depths in the skull because of stepwise decreasing shunting currents.

stimulation) in one patient, data of 10 patients (6f, 53 ± 11 years) were included in the analysis.

Accuracy of the stimulator and measurements

The stimulator showed a mean error of 0.6 mA between the preset value of the stimulation current and the measured current. The first and second measurements were in average reproducible within ±1.5% for CMT; within ±6% for VMT, and within ±6.3% for impedance (Table 2). Thus, further data analysis could be performed with the first measurements.

Stimulation intensities and impedances

Fig. 3 shows a typical example of simultaneously measured voltage and current pulse series as obtained from the set-up as in Fig. 1. The current pulses are rectangular, except for small overshoots at the transitions from off to on and vice versa. There are no visible build-up effects since the after effects in both the current and voltage graphs in Fig. 3A and B respectively are died out completely at the onset of subsequent pulses. Because of the high reproducibility of all pulses, one can consider the current and voltage readings from the first pulse to represent all others. The enlarged first current and voltage pulse in Fig. 3C and D show that the choice of taking the current and voltage readings in the middle of the pulse is at a stationary plateau where the initial distortions of the overshoot of the current and gradual increase of the voltage due to the capacitive effects are cleared. Average CMTs, VMTs and impedances are presented in Table 2. When stimulating with the monopolar probe on the skin, CMTs were 55 ± 28 mA (Table 2). CMT values for the stepwise stimulation at each of the 8 subsequent layers between the skin surface and the cerebral cortex expressed in percentage of this averaged CMT were as follows: CS 98%; within the scalp 106%; OCL 60%; SL 60%; ICL 51%; dura 46% and cortex 24%. Impedance was highest for all skull layers (OCL, SL and ICL) and lowest for stimulation with CS-electrodes and on the dura (ED).

Cross comparison for CMT revealed significance between the stimulation on the cortex and CS, skin, scalp and ICL, as well as between the stimulation with CS and ICL and skin (Table 3). CMT for all other layers did not show any significant correlation. This lack of significance is in agreement with the larger overlap of the SEM regions indicated in Table 2.

Correlation between CMT, VMT and impedance

In Table 4 correlations between CMT, VMT and impedance for the 8 successive layers between the skin surface and the cerebral cortex are given.

VMT and CMT were only significantly correlated (correlation > 0.7) for stimulation with the monopolar probe on the skin, the SL and cortex with a level of significance $P < 0.05$. This is explained by the low figures of numbers. CMT and impedance were only significantly correlated for the OCL. The correlation between VMT and impedance was higher for complimentary locations when compared to the correlation between CMT and VMT: it was significant for the skull bone layer OCL ($P < 0.05$), but not for SL and ICL.

Discussion

Accuracy of the measurements

In individual measurements, there are no build-up effects in the voltage and current pulses that need further discussion. The influence of tissue capacitance is only visible in the first 10–20 μs after the onset of pulses. Since the pulses in a train reproduce themselves, one can consider the first pulse to represent them all whereas the readings of the threshold currents and voltages at the middle of the curve represent the resistive part of the impedance when capacitive effects have subsided. When compared to inter-individual differences in the measurements, the accuracy of the current stimulator and the reproducibility of the measurements are sufficient to use the first measurements only in data analysis. When omitting the initial glitch of the current in the first microsecond of the current pulse as shown in Fig. 3A and C, the reading from the horizontal part of the rectangular pulse from the oscilloscope is usually within the step size of 1 mA of the selected current of the stimulator when the output was well within the voltage limit.

However, the current stimulator's limited voltage range of 300 V is a technical restriction to be considered: when impedance exceeds 5 kΩ and MEPs could not be elicited and then the threshold current cannot be delivered and in consequence not be measured. This occurred at dry conditions of the contact surfaces of skin, skull layers and dura. Exclusion of measurements resulting from those conditions may have caused unknown underestimation of stimulation voltage and impedance of the two compact bone layers. Local

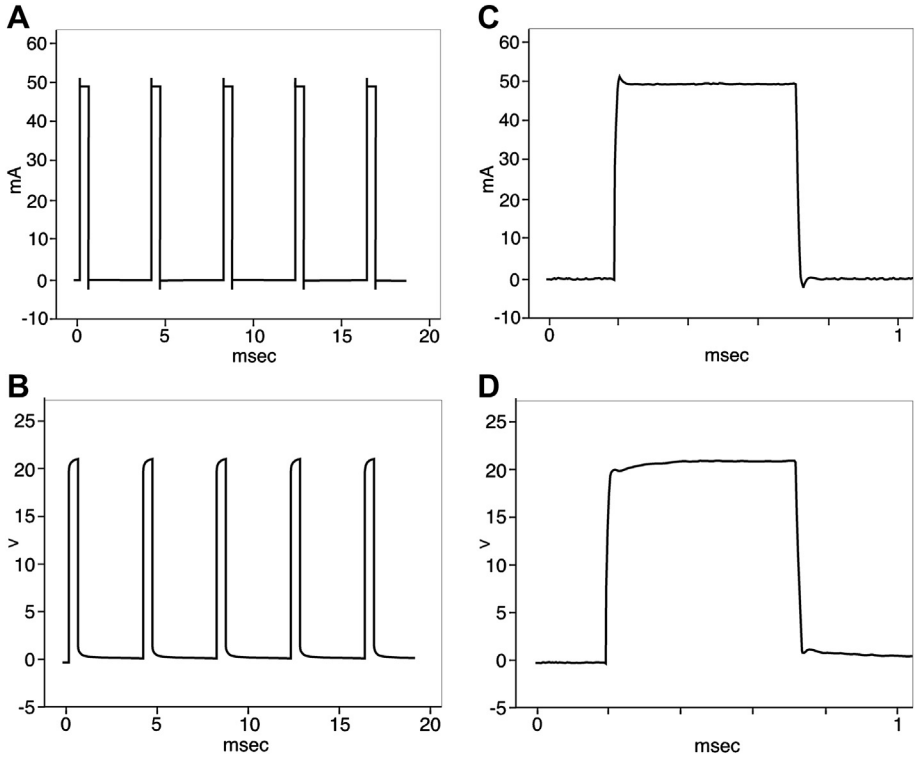

Figure 3. Example of simultaneous measured pulse current (A) and pulse voltage (B). The upper panels show the first four pulses of a 5 pulse TES train series. The data are taken from case 5, anodal probe at scalp location with a current threshold of 49 mA. Pulse width is 0.5 ms; interpulse interval (time between the onset of each pulse) is 4 ms. Rectangular pulses are delivered by a current stimulator. This typical example shows no visible build-up effects in current as well as the current series. C is the enlarged first current pulse and D the enlarged first voltage pulse. At the middle of the pulses, the currents are stable and used for computations.

impedance decreases by administering saline drops close to the anode as this enlarges the virtual contact surface of the ball tip electrode. Moisture and hydration of the skull bone also has a substantial effect on the conductivity: a dry human skull has a 4–10 times lower conductivity compared to a skull soaked in saline [11,26].

Stimulation intensities and impedances

The CMT decreased by 37% between the scalp and the three bone layers and by 60% for the stimulation on the scalp and on the dura (Table 2). This indicates that about half of the current is shunted by the scalp. Due to the relatively poor conductivity of the skull layers, the shunting currents are expected to flow mainly from the stimulation electrode through the scalp and CSF. The relatively small and gradual decrement of the CMT from the OCL (−8 mA (OCL to ED)), SL (−8 mA (SL to ED)) and ICL (−3 mA (ICL to ED)) to the dural layer is indicative for current bypassing the higher resistance of the skull. Superior conductivity of the SL could be explained by the virtual increase of the anodal contact surface which may result from a plastic deformation of the soft and fluid immersed SL due to pressure on the electrode. Studying the in vitro conductivity of vital human skull layers indicated a 4–6 times higher conductivity of the SL (16.2–41.1 milli-Siemens per meter (mS/m)) compared to the OCL (4–7.2 mS/m) and ICL (2.8–10.2 mS/m) [19]. The smaller differences of the mean CMTs between the bone and dural layers are therefore not statistically significant.

Table 1
Characteristics of patients' included into data analysis.

Pat.	Gender	Age	Location	Side	Histology
1	F	67	Temporal	Left	GBM
2	F	54	Parasaggital-precentral	Right	Oligoastroytoma
3	M	53	Parasaggital-precentral	Bilateral	Meningeoma
4	F	54	Temporal	Left	GBM
5	F	56	Parietal	Right	Meningeoma
7	F	64	Fronto-central	Left	Meningeoma
8	F	59	Parietal	Left	Meningeoma
9	M	41	Temporal	Left	Astrocytoma
10	M	31	Insular	Left	Astrocytoma
11	M	48	Postcentral	Right	Astrocytoma

Patient 6 was excluded due to technical constraints.

Motor thresholds of direct cortical stimulation

The stimulation intensities that were necessary to elicit MEPs by direct cortical stimulation might be considered relatively high. Due to the study design, the burr hole was determined by a tailored craniotomy and not the optimal location for direct cortical mapping over the hand motor cortex area. As direct cortical stimulation is focal, its intensity depends markedly on the stimulation location. This explains a bias towards higher stimulation intensities in our series. Ideally, the intensity of direct cortical stimulation ranges between 5 and 16 mA [4,23,27,28]. The relation between the extraccortical and cortical motor threshold currents can be defined as a ratio of $CMT_{cortex}/CMT_{extracortical}$. For stimulation at the C3-anode and C4-anode the range of this ratio lies between 10% and 25%. When the extracranial electrodes are placed closer to each other their CMTs are higher [15]. This will result in a lower range of this ratio.

Correlation between CMT, VMT and impedance

Low stimulation electrode impedances

When electrode impedances were relatively low, there was a significant correlation between the VMT and CMT (0.72–0.89 at

Table 2
Mean, standard deviation (SD), standard error of mean (SEM) and the mean reproducibility error (mRE) of the CMT, VMT and impedance.

Location	Type of stimulation electrode	Number of values	CMT (mA)				VMT (V)				Impedance R_{el} (Ω)			
		N	Mean	SD	SEM	mRE %[b]	Mean	SD	SEM	mRE %[b]	Mean	SD	SEM	mRE %[b]
Skin	Corkscrew electrode	9	54.2	22.8	7.6	1.9	38.1	20.7	6.9	−0.4	686	146	49	−1.1
On skin	Monopolar probe	9	55.3	27.9	9.3	4.4	99.9	43.5	14.5	1.5	1911	683	228	3.5
Scalp[a]	Monopolar probe	6	58.8	32.1	13.1	−1.6	56.3	28.4	11.6	−0.1	1010	402	164	−1.6
OCL	Monopolar probe	9	33.2	23.1	7.7	−4.1	91.3	53.1	17.7	−0.02	3734	2793	931	−4.4
SL	Monopolar probe	10	33.4	22.5	7.3	0.3	70.2	44.3	14.0	0.1	2347	1327	420	0.2
ICL	Monopolar probe	10	28.4	18.7	5.9	6.0	48.1	22.5	7.1	−0.1	2103	1498	474	6.3
ED	Monopolar probe	5	25.4	12.3	5.5	−5.5	17.2	11.6	5.2	0	642	244	109	−0.8
Cortex	Monopolar probe	6	13.5	5.9	2.4	1.4	11.4	5.4	2.4	0	859	300	122	1.8

CMT = current intensity at motor threshold; VMT = voltage intensity at motor threshold; OCL = outer compact layer of the skull; SL = spongeous layer; ICL = inner compact layer; ED = epidural level; cortex = on the cortex.
[a] Within the skin of the scalp after incision.
[b] mRE% was computed from the two subsequent measurements of each stimulation site.

a significance level of 0.05; Table 4) rendering both potentially useful in determining stimulation thresholds, markedly unaffected by impedance at extracranial as well as intracranial electrode positions. Indeed, voltage stimulation has been successfully described for extracranial stimulation [6,12]. Furthermore, subthreshold motor cortex stimulation either by constant voltage or constant current stimulation has been applied for epidural motor cortex stimulation in treatment of pain or motor disorders in Parkinson's disease, where therapeutic stimulation intensities are referenced to motor thresholds [26,29,30]. However, once stationary conditions are achieved, as is the case for implanted electrodes voltage stimulation might be used. However, in intraoperative neuromonitoring, where surgical manipulations and effects of prolonged anesthesia and positioning may inadvertently affect impedance, current stimulation is preferable due to its lower sensitivity to impedance.

High stimulation electrode impedances

In the case of relatively high or markedly drifting electrode impedances the use of voltage stimulators is discouraged. As noticed for the skull layers, the stimulation situation is completely different for high electrode impedances when compared to low electrode impedances. According to Table 4, significant correlation between the impedance and VMT was seen for CS, ICL and on the dura. On the contrary, there was no correlation between CMT and impedance except for OCL. This calls for the use of current stimulators in favor of voltage stimulators in order to minimize the dependence on impedance when impedances are relatively high.

Comparison of results to an experimental model and review of literature

The decreasing CMT found from the scalp, along the layers to the cortex can be explained with a "current peeling principle" (Fig. 2). This gives insight in the fractions of parallel shunted currents being injected into the different tissue layers. The peeling principle is based on the assumption that the total amount of current equals the sum of current injected in each separate layer and finally the brain tissue harboring the pyramidal axons to be depolarized. However, this simplification introduces an inaccuracy: the electrical field in the layers under the stimulating electrode alters at each electrode position and does not remain the same as depicted in Fig. 2. The current paths and densities in cortical and subcortical regions will change as well at stepwise penetration of the electrode. A far-field configuration involved in extracranial stimulation depolarizes a larger population of axons over a wide somatotopic range within a cortical area covering a radius of several centimeters, whereas stimulation on the cortex or just below resembles near field conditions. In these conditions, stimulation occurs within a diameter of several millimeters, which is smaller than the accepted 1 cm distance between the burr-hole and the expected cortical representation of the abductor pollicis brevis muscle. Therefore the CMTs and VMTs of direct cortical stimulation may be overestimated.

Current spreading

Currents spread preferentially along routes with highest conductance. The current is not strictly bounded to the specific layer into which it is injected. When a current is injected into one of the poorly conducting skull layers, most of the current will divert into the well-conducting subdural CSF and the scalp layer as shown in Fig. 2B–D and will avoid the inner and outer compact layers (Fig. 2B and D). This explains the stepwise decrease of CMTs on penetration of the electrode. Also our results justify the observation by Watanabe et al. that placement of screw-electrodes within skull bone can significantly reduce stimulation intensity to elicit MEPs [21]. This significant reduction of the CMT of "in-bone-stimulation" can be ascribed to a marked reduction of current conduction in the

Table 3
Cross comparison of CMT obtained at stepwise stimulation at 8 layers along a tract between the skin surface and cerebral cortex.

Stimulation		Cortex		ED		ICL		SL		OCL		Scalp[a]		Skin	
Type of electrode	Location	t	s	t	s	t	s	t	s	t	s	t	s	t	s
Corkscrew	Skin	−3.9	**0.02**	−2.3	0.09	−4.0	**<u>0.01</u>**	−1.9	0.10	−1.7	0.14	0.23	0.83	0.14	0.89
Monopolar stimulation probe	Skin	−4.4	**<u>0.01</u>**	−2.6	0.06	−5.2	**<u>0.01</u>**	−1.8	0.11	−1.6	0.15	0.40	0.70		
	Scalp[a]	−4.2	**<u>0.01</u>**	−1.8	0.15	−1.8	0.14	−1.0	0.36	−0.9	0.40				
	OCL	−2.1	0.10	−1.3	0.27	−0.4	0.69	−1.9	0.09						
	SL	−2.0	0.11	−1.2	0.32	0.20	0.85								
	ICL	−3.5	**0.03**	−0.9	0.42										
	ED	−1.8	0.15												

CMT = current intensity at motor threshold; OCL = outer compact layer of the skull; SL = spongeous layer; ICL = inner layer; ED = epidural level.
Pairs of t- and 2-tailed significance values for 8 levels of stimulation locations are presented. Levels of significance: ≤5%: bold; ≤1%: bold and underlined; student's *t*-test (paired).
[a] Within the skin of the scalp.

Table 4
Spearman's correlation coefficients of three combinations of CMT, VMT and impedance for stepwise stimulation at 8 layers along a tract between the skin surface and cerebral cortex.

Spearman's correlation								
Stimulation			CMT − VMT		CMT − Impedance (R_{el})		VMT − Impedance (R_{el})	
Electrode type	Location	*N*	Correlation	Significance level	Correlation	Significance level	Correlation	Significance level
CS	Skin	9	0.60	0.08	0.14	>0.5	**0.68**	0.04
Mono-polar probe	Skin	9	**0.72**	**0.03**	<0.001	>0.5	0.58	0.1
	Scalp[a]	6	0.77	0.08	−0.26	>0.5	0.37	0.46
	OCL	9	−0.13	>0.5	**−0.84**	0.04	0.60	0.08
	SL	10	**0.72**	**0.02**	−0.18	>0.5	0.48	0.16
	ICL	9	0.17	>0.5	−0.53	0.14	**0.68**	0.04
	ED	5	0.80	0.1	0.60	0.28	**0.90**	0.04
	Cortex	6	**0.89**	0.02	−0.14	>0.5	−0.03	>0.5

CS = corkscrew electrode; OCL = outer compact layer of the skull; SL = spongeous layer; ICL = inner layer; ED = epidural level; *N* = sample size (sample size for ICL differs from the one mentioned in Table 2 as all three the values of VMT, CMT and impedance R_{el} were only present in 9 cases).
Bold: correlation is significant at the 0.05 level (2-tailed).
[a] Within the scalp after incision.

scalp. Any changes in the characteristics of the scalp conductivity will still influence the CMT, even when electrodes are placed in the skull. This is of relevance in scalp edema to which CMT is highly susceptible. If the development of a significant scalp edema is of concern, alternatively voltage stimulation using subdermal large surface needle electrodes with low impedances may be considered [12]. Under ideal circumstances, voltage stimulators are not sensitive to changes in parallel conduction in the scalp layer.

Spatial resolution of stimulation

Placement of screw-electrodes within the skull bone is expected to allow a higher spatial resolution because of the decreased distance to the cortex. However, the unknown distribution of current through the skull layers to the CSF and back to the scalp may decrease the spatial selectivity of a close field. Therefore it remains unclear if the spatial resolution of extracranial electrodes is improved by placing electrodes into the skull – as suggested by Watanabe et al. [21]. Thus, the main characteristics of stimulation within the skull are not only lower motor thresholds due to lower stimulation intensity but also a reduced extracranial current conduction.

Theoretically, a reduction of current conduction through the scalp layer would imply decreased extracranial currents that may be responsible for the generation of unwanted M-responses (i.e. muscle responses due to direct stimulation of peripheral axons). This would result in increased M-response thresholds. Low M-response thresholds might complicate monitoring of corticobulbar MEPs [30]. As such skull screws theoretically could offer a solution to this problem. The drawbacks of the clinical use of skull screws for stimulation are the invasiveness of the method with the accompanying risk of infection, the unavailability of CE- or FDA certified stimulation screws and the limitation in the amount of electrodes locations. To our opinion, this does not outweigh the potential clinical advantages in monitoring above common TES with subcutaneous needle electrodes.

One also has to consider whether the underlying pathology may influence the measurements. Theoretically, an intrinsic growing intracerebral lesion might differ from extrinsic brain tumors especially if the latter infiltrate the bone, e.g. meningiomas or osteomas. In none of the studied patients, the part of the skull in which the measurements were performed was infiltrated by a meningioma. To further study the effect of underlying pathology a larger cohort is necessary.

Recommendation for choice of voltage and current stimulators

This study demonstrates that both voltage and current stimulators are useful for threshold measurements, except for in the two compact bone layers. Regardless whether extracranial or intracranial stimulation is used, the voltage or current thresholds for MEPs, may depend on changes in conductivity of several volume conductors through which the induced current flows. In this perspective, the choice toward the use of voltage or current stimulators might be difficult. The observed high correlations between voltage and current threshold experiments and relative insensitivity to impedance are present when the local electrode impedances are relatively low. In addition, it supports the high correlation between specifically voltage stimulation and electrode impedance when local impedances are high as seen in the skull layers in Table 3. When impedances are not exceeding for the voltage range of a current stimulator, current stimulation remains the optimal choice in case of high electrode impedances. For transcranial, epidural and direct cortical stimulation using standard electrodes, the choice between voltage and current stimulation becomes less critical in everyday practice, unless specific impedance changes are more or less predictable. For example, in motor cortex stimulation with implanted electrodes the thickness of the subdural CSF layer may vary due to changes in position of the patient.

Conclusion

The study demonstrates a stepwise reduction of the mean stimulation current of the CMT along the extracranial to cortical anodal trajectory which is explained by successive exclusion of layerbound shunting currents. Remarkably, low CMTs were encountered within the skull layers in comparison to TES that implies relatively strong shunting currents in the scalp layer. The measurements showed a strong dependence of the VMT on electrode impedance for the three skull layers and to a lesser extent on the stimulation locations at the skin which revealed relatively high impedance. These conditions favor the use of constant current stimulation, unless electrodes with large contact surfaces are used.

In everyday clinical practice of stimulation to elicit MEPs the choice of voltage or current stimulators become less relevant. When changes in parallel conduction are expected, voltage stimulators may prevail whereas current stimulators are advised when predominant changes in local electrode impedances are predicted.

Acknowledgment

The design and application of the measuring set-up was developed in cooperation with the Medical Electronic Department of the Sint Maartenskliniek, Nijmegen, The Netherlands.

References

[1] Neuloh G, Schramm J. Monitoring of motor evoked potentials compared with somatosensory evoked potentials and microvascular Doppler ultrasonography in cerebral aneurysm surgery. J Neurosurg 2004;100:389–99.

[2] Neuloh G, Pechstein U, Cedzich C, Schramm J. Motor evoked potential monitoring in supratentorial surgery. Neurosurgery 2004;54:1061–72.
[3] Neuloh G, Pechstein U, Schramm J. Motor tract monitoring during insular glioma surgery. J Neurosurg 2007;106:582–92.
[4] Szelenyi A, Kothbauer K, de Camargo AB, Langer D, Flamm ES, Deletis V. Motor evoked potential monitoring during cerebral aneurysm surgery: technical aspects and comparison of transcranial and direct cortical stimulation. Neurosurgery 2005;57:331–8.
[5] Szelenyi A, Langer D, Kothbauer K, Camargo AB, Flamm ES, Deletis V. Motor evoked potentials monitoring during cerebral aneurysm surgery: intraoperative changes and postoperative outcome. J Neurosurg 2006;105:675–81.
[6] Calancie B, Harris W, Broton JG, Alexeeva N, Green BA. "Threshold-level" multipulse transcranial electrical stimulation of motor cortex for intraoperative monitoring of spinal motor tracts: description of method and comparison to somatosensory evoked potential monitoring. J Neurosurg 1998;88:457–70.
[7] Kothbauer K, Deletis V, Epstein F. Motor-evoked potential monitoring for intramedullary spinal cord tumor surgery: correlation of clinical and neurophysiological data in a series of 100 consecutive procedures 1998;1–9. http://www.aans.org/education/journal/neurosurgical/may98/4-5-1.asp.
[8] Taniguchi M, Cedzich C, Schramm J. Modification of cortical stimulation for motor evoked potentials under general anesthesia: technical description. Neurosurgery 1993;32:219–26.
[9] Li DL, Journee HL, van Hulzen A, Rath WT, Sclabassi RJ, Sun M. Computer simulation of corticospinal activity during transcranial electrical stimulation in neurosurgery. Stud Health Technol Inform 2007;125:292–7.
[10] Roth BJ, Saypol JM, Hallett M, Cohen LG. A theoretical calculation of the electric field induced in the cortex during magnetic stimulation. Electroencephalogr Clin Neurophysiol 1991;81:47–56.
[11] Nathan SS, Sinha SR, Gordon B, Lesser RP, Thakor NV. Determination of current density distributions generated by electrical stimulation of the human cerebral cortex. Electroencephalogr Clin Neurophysiol 1993;86:183–92.
[12] Journee HL, Polak HE, de Kleuver M. Influence of electrode impedance on threshold voltage for transcranial electrical stimulation in motor evoked potential monitoring. Med Biol Eng Comput 2004;42:557–61.
[13] Deletis V, Isgum V, Amassian VE. Neurophysiological mechanisms underlying motor-evoked potentials in anesthetized humans. Part 1. Recovery time of corticospinal tract waves elicited by pairs of transcranial electrical stimulation. Clin Neurophysiol 2001;112:438–44.
[14] Deletis V, Rodi Z, Amassian VE. Neurophysiological mechanisms underlying motor-evoked potentials in anesthetized humans. Part 2. Relationship between epidurally and muscle recorded MEPs in man. Clin Neurophysiol 2001;112:445–52.
[15] Szelenyi A, Kothbauer KF, Deletis V. Transcranial electric stimulation for intraoperative motor evoked potential monitoring: stimulation parameters and electrode montages. Clin Neurophysiol 2007;118:1586–95.
[16] Calancie B, Harris W, Brindle GF, Green BA, Landy HJ. Threshold-level repetitive transcranial electrical stimulation for intraoperative monitoring of central motor conduction. J Neurosurg 2001;95:161–8.
[17] Oostendorp TF, Delbeke J, Stegeman DF. The conductivity of the human skull: results of in vivo and in vitro measurements. IEEE Trans Biomed Eng 2000;47:1487–92.
[18] Hoekema R, Wieneke GH, Leijten FS, van Veelen CW, van Rijen PC, Huiskamp GJ, et al. Measurement of the conductivity of skull, temporarily removed during epilepsy surgery. Brain Topogr 2003;16:29–38.
[19] Akhtari M, Bryant HC, Mamelak AN, Flynn ER, Heller L, Shih JJ, et al. Conductivities of three-layer live human skull. Brain Topogr 2002;14:151–67.
[20] Akhtari M, Bryant HC, Emin D, Merrifield W, Mamelak AN, Flynn ER, et al. A model for frequency dependence of conductivities of the live human skull. Brain Topogr 2003;16:39–55.
[21] Watanabe K, Watanabe T, Takahashi A, Saito N, Hirato M, Sasaki T. Transcranial electrical stimulation through screw electrodes for intraoperative monitoring of motor evoked potentials. Technical note. J Neurosurg 2004;100:155–60.
[22] Kombos T, Suess O, Kern BC, Funk T, Hoell T, Kopetsch O, et al. Comparison between monopolar and bipolar electrical stimulation of the motor cortex. Acta Neurochir (Wien) 1999;141:1295–301.
[23] Kombos T, Suess O, Funk T, Kern BC, Brock M. Intra-operative mapping of the motor cortex during surgery in and around the motor cortex. Acta Neurochir (Wien) 2000;142:263–8.
[24] Szelenyi A, Langer D, Beck J, Raabe A, Flamm ES, Seifert V, et al. Transcranial and direct cortical stimulation for motor evoked potential monitoring in intracerebral aneurysm surgery. Neurophysiol Clin 2007;37:391–8.
[25] Merrill DR, Bikson M, Jefferys JG. Electrical stimulation of excitable tissue: design of efficacious and safe protocols. J Neurosci Methods 2005;141:171–98.
[26] Arle JE, Shils JL. Motor cortex stimulation for pain and movement disorders. Neurotherapeutics 2008;5:37–49.
[27] Cedzich C, Taniguchi M, Schafer S, Schramm J. Somatosensory evoked potential phase reversal and direct motor cortex stimulation during surgery in and around the central region. Neurosurgery 1996;38:962–70.
[28] Kombos T, Suess O, Ciklatekerlio O, Brock M. Monitoring of intraoperative motor evoked potentials to increase the safety of surgery in and around the motor cortex. J Neurosurg 2001;95:608–14.
[29] Cioni B, Meglio M, Perotti V, De Bonis P, Montano N. Neurophysiological aspects of chronic motor cortex stimulation. Neurophysiol Clin 2007;37:441–7.
[30] Holsheimer J, Lefaucheur JP, Buitenweg JR, Goujon C, Nineb A, Nguyen JP. The role of intra-operative motor evoked potentials in the optimization of chronic cortical stimulation for the treatment of neuropathic pain. Clin Neurophysiol 2007;118:2287–96.